GLIA 56:97–105 (2008)

Inhibition of Injury-Induced Glial Aromatase Reveals a Wave of Secondary Degeneration in the Songbird Brain

RYAN D. WYNNE,[1] BRADLEY J. WALTERS,[1] DAVID J. BAILEY,[1] AND COLIN J. SALDANHA[1,2]*
[1]*Department of Biological Sciences, Lehigh University, Bethlehem, Pennsylvania*
[2]*Program in Cognitive Science, Lehigh University, Bethlehem, Pennsylvania*

KEY WORDS
gliosis; neuroprotection; estrogen; apoptosis; necrosis; stroke

ABSTRACT
Mechanical or anoxic/ischemic brain insult results in reactive gliosis and a pronounced wave of apoptotic secondary degeneration (WSD). Reactive glia express aromatase (estrogen synthase) and glial estrogen synthesis decreases apoptosis and the volume of degeneration. Whether aromatization by glia affects gliosis itself or the initiation/maintenance of the WSD remains unknown. Adult male zebra finches (*Taeniopygia guttata*) were injured with a needle that contained the aromatase inhibitor fadrozole or vehicle into contralateral hemispheres. Birds were killed at 0, 2, 6, 24, 72 h, 2 or 6 weeks postinjury. Gliosis and degeneration were measured with vimentin- and Fluoro-Jade B-expression, respectively. Reactive gliosis was detectable at 6 h, reached asymptote at 72 h, and continued until 6 weeks postinsult. Gliosis extended further around fadrozole-injury than vehicle, an effect driven by a larger area of gliosis around fadrozole- relative to vehicle-injury at 72 h postinsult. Glial aromatase was inhibited for about 2 weeks postinjury since aromatase relative optical density was higher around fadrozole-injury relative to vehicle-injury until this time-point. Degeneration around vehicle-injury reached asymptote at 2 h postinsult, but that around fadrozole-injury peaked 24–72 h postinjury and decreased thereafter. Thus, the injury-induced WSD as described in mammals is detectable in zebra finches only following glial aromatase inhibition. In the zebra finch, injury-induced estrogen provision may decrease reactive gliosis and severely dampen the WSD, suggesting that songbirds are powerful models for understanding the role of glial aromatization in secondary brain damage.

INTRODUCTION

Injury to the homeotherm brain results in reactive astrogliosis (McGraw et al., 2001; Sofroniew, 2005). The role of reactive gliosis in the isolation of damage from healthy neuropil and the promotion of regenerative events are areas of intense investigation (Liberto et al., 2004; Pekny and Nilsson, 2005; Pekny et al., 1999). Astrocytic responses to brain injury include cell proliferation, hypertrophy, changes in gene expression, and the secretion of pro- and anti-inflammatory cytokines (Chen and Swanson, 2003; Eddleston and Mucke, 1993; Eng and Ghirnikar, 1994; Liberto et al., 2004; Pekny and Nilsson, 2005; Ridet et al., 1997; Sofroniew, 2005; Swanson et al., 2004). Notable in the physiological parameters affected by gliosis is a profound effect of glia on secondary degeneration (Liberto et al., 2004; Liu et al., 1999; Myer et al., 2006).

In mammals, brain injury is followed by a wave of apoptotic secondary degeneration (WSD; Arvin et al., 1996; Benkovic et al., 2004, 2006; Butler et al., 2002; Carswell et al., 2005; Chen and Swanson, 2003; Chen et al., 2004; Clark et al., 1993; Darsalia et al., 2005; Garcia-Ovejero et al., 2005; Jorgensen et al., 1993; Pekny and Nilsson, 2005; Sato et al., 2001; Wise et al., 2005). Secondary degeneration peaks 24 h postinsult, but remains detectable for up to 30 days. This WSD is hypothesized to be responsible for the many symptoms associated with brain damage (for review see Mattson et al., 2000). The amplitude of the WSD at various discrete time-points is affected by numerous factors including cations, cytokines, adhesion molecules, and steroid hormones (Arvin et al., 1996; Liberto et al., 2004; Mrak and Griffin, 2005).

Estrogen (E) appears to be a potent mitigator of secondary degeneration (Rau et al., 2003a,b; Suzuki et al., 2006; Wise, 2006). E-replacement decreases apoptosis (Rau et al., 2003a) and decreases cell death by upregulating the proto-oncogene Bcl-2 (Dubal et al., 1999). E also protects neurons against degeneration caused by serum deprivation (Green et al., 1996), glutamate exposure (Mize et al., 2003), or mechanical injury (Garcia-Segura et al., 2001).

Es are synthesized in the male and female brain via aromatase (E-synthase; Balthazart et al., 1990; Goodson et al., 2005; MacLusky and Naftolin, 1981; Schlinger, 1997). In mammals and birds, aromatase is constitutively expressed in neurons (Balthazart et al., 1990; Negri Cesi et al., 1992; Schlinger, 1997). However, injury to the avian and mammalian brain induces aromatase expression in glia (Azcoitia et al., 2003; Garcia-Segura et al., 1999; Peterson et al., 2001, 2004; Saldanha et al., 2005; Wynne and Saldanha, 2004). This upregulation limits degeneration via local E synthesis (Saldanha et al., 2005). Studies in mammals demonstrate increased injury size following central administration of aromatase inhibitors (Azcoitia et al., 2003) and in aromatase-knockouts relative to

Grant sponsor: NIH NS; Grant number: 042767.

*Correspondence to: Colin J. Saldanha, Deptartment of Biological Sciences, Lehigh University, 111 Research Drive, Bethlehem, PA 18015, USA.
E-mail: colin@lehigh.edu

Received 18 June 2007; Accepted 10 September 2007

DOI 10.1002/glia.20594

Published online 22 October 2007 in Wiley InterScience (www.interscience.wiley.com).

controls (Azcoitia et al., 2001). Peripheral administration of E or aromatizable androgens decreases injury size in rats (Garcia-Segura et al., 2003). These results suggest a critical role for glial aromatization in limiting degeneration following insult to the homeotherm brain. Whereas several studies have documented the actions of aromatase on degeneration at discrete points following injury, fewer have asked if glial aromatase affects the initiation and/or maintenance of the WSD.

Songbirds are excellent models for these studies as neuronal aromatase is abundant, yet constrained to several telencephalic regions (Goodson et al., 2005; Schlinger, 1997). Further, injury rapidly upregulates glial aromatase expression (Peterson et al., 2001, 2004; Saldanha et al., 2005; Wynne and Saldanha, 2004). Glial aromatization inhibits apoptosis and decreases neural injury size (Saldanha et al., 2005; Wynne and Saldanha, 2004). However, the role of injury-induced glial aromatase on the dynamics of the WSD in songbirds remains uninvestigated.

In this study, we tested the effect of aromatase inhibition on reactive gliosis and the dynamics of the WSD in the adult male zebra finch brain. We show that inhibition of aromatase increases reactive gliosis and that the WSD characteristic of brain injury in most mammals is only detectable following aromatase inhibition in the zebra finch.

MATERIALS AND METHODS

Subjects

Thirty-three adult (>90 days posthatching) male zebra finches were purchased from a breeder (Canary Bird Farms, Old Bridge, NJ) and housed in the Biological Sciences Animal Facility, Lehigh University. Birds were held in same-sex groups (3–4 per group) in cages (18″ × 18″ × 16″) under a 14:10 LD cycle (lights on at 0600 h). Room temperature was maintained at 72°F ± 2°F and food, grit, water, and cuttlebones were available *ad libitum*. All housing and experimental protocols used were approved by the Lehigh University Institutional Animal Care and Use Committee (IACUC).

Neural Injury and Drug Delivery

Subjects were anesthetized (0.08 mL of 16 mg/mL ketamine and 0.3 mg/mL xylazine in 0.9% saline) and positioned in a stereotaxic apparatus with the head angled at 45°. The cranium was exposed and an 18G needle was used to create a bilateral craniotomy 2-mm anterior to the pineal gland and 3-mm lateral to the midline. Injections were targeted toward the entopallial nucleus 3-mm ventral to the brain surface (Stokes et al., 1974), because it lacks constitutively expressed neuronal aromatase (Saldanha et al., 2000, 2005; Shen et al., 1995; Wynne and Saldanha, 2004). A 50-μL 22s Hamilton syringe (Hamilton Company, Reno, NV) was positioned at the surface of the brain at an angle of 45° and lowered to the target where it remained for 120 s. At this point, 5 μL of a 10 mg/mL solution of the aromatase inhibitor fadrozole (50 μg total; Wade et al., 1994) in 0.9% saline was injected into one hemisphere and 0.9% saline (vehicle) was injected into the contralateral hemisphere of the same bird. The needle remained in the brain for 60 s before retraction. The scalp was sealed with Collodion Flexible (EM Science, Gibbstown, NJ). Birds recovered from anesthesia under a heat lamp and were killed at the time-points indicated.

Tissue Preparation

Birds were killed via decapitation 2, 6, 24, 72 h, 2 or 6 weeks postsurgery. Three subjects were killed immediately following sealing of the scalp (0-h time-point). Brains were removed and immersed in 5% acrolein in 0.1 M phosphate buffered-saline, pH = 7.4 (PBS). Brains were agitated overnight in fixative at room temperature, rinsed 4 × 15 min with 0.1 M PBS, embedded in 8% gelatin, re-immersed and cryoprotected in 5% acrolein/30% sucrose in 0.1 M PBS for 72 h at 4°C, washed in 30% sucrose for 24 h at 4°C, and sectioned on a cryostat. Five sets (A–E) of 50-μm coronal sections were collected into a high-sucrose, polyethylene glycol solution (Watson et al., 1986) and stored at −20°C. Sets of sections were used to determine (a) reactive gliosis using vimentin expression (Alvarez-Buylla et al., 1987), (b) the effectiveness of fadrozole using the intensity of aromatase immunoproduct (Saldanha et al., 2000, 2005; Wynne and Saldanha, 2004), and (c) cellular degeneration using Fluoro-Jade B (Schmued and Hopkins, 2000). Other sets of sections were used to optimize protocols or as replicates.

Vimentin Expression

We used an antibody previously characterized to specifically bind vimentin in the avian brain (Alvarez-Buylla et al., 1987; Saldanha et al., 2005). Sections were exposed to 0.1 M phosphate buffer (PB; 6 × 15 min), 1% sodium borohydride in 0.1 M PB (30 min), 0.1 M PB containing 0.1% Triton X-100 (0.1% PBT; 3 × 15 min), 10% normal goat serum in 0.3% PBT (60 min), and 1:750 anti-vimentin (Developmental Studies Hybridoma Bank, Iowa City, IA) in 0.3% PBT (48 h) at 4°C. Sections were exposed to 0.1% PBT (6 × 15 min), 1:50 rat-adsorbed goat anti-mouse cyanine-5 (CY-5; Jackson Immunochemicals, West Grove, PA) in 0.3% PBT (24 h) at 4°C under foil, 0.1% PBT (6 × 15 min), mounted, dehydrated, and coverslipped.

Aromatase Expression

We used an antibody previously characterized using absorption, no-primary, and Western blot analysis (Saldanha et al., 2000, 2005). Sections were exposed to 0.1 M phosphate buffer (PB; 6 × 15min), 1% sodium borohydride in 0.1 M PB (30 min), 0.1% PBT (3 × 15 min), 10% normal goat serum in 0.3% PBT (60 min), and 1:2,500 AZAC (48 h) at 4°C. Sections were then exposed to 0.1% PBT (6 × 15 min), 1:50 rat-adsorbed goat anti-rabbit cya-

nine-5 in 0.3% PBT (24 h) at 4°C under foil, 0.1% PBT (6 × 15 min), mounted, dehydrated, and coverslipped.

Cellular Degeneration

We used Fluoro-Jade B, a poly-anionic fluroescein derivative hypothesized to bind to positively charged molecules in dying neurons and glia (Anderson et al., 2003; Butler et al., 2002; Saldanha et al., 2005; Schmued and Hopkins, 2000). Sections were mounted onto subbed slides, air dried for 24 h, and exposed to 1% sodium hydroxide in 80% ethanol (5 min), 70% ethanol (2 min), distilled water (2 min), 0.06% potassium permanganate (10 min), distilled water (2 min), and stained with 0.0004% Fluoro-Jade B (Chemicon, Temecula, CA; 20 min) under low light conditions. Sections were then rinsed in distilled water (3 × 1 min), air dried, cleared with xylene, and coverslipped.

Confocal Microscopy

Sections stained with antibodies against vimentin and aromatase and those stained with Fluoro-Jade B were examined under a scanning confocal microscope (Zeiss LSM510). Sections were observed under 5×, 25×, or 63×/1.4 NA plan apo objectives. Argon ion, 543 HeNe and 633 HeNe lasers were used to generate the 543 (Fluoro-Jade B) and 633 (CY-5) lines used for excitation, and pinholes were set to 1–1.5 airy units. Regardless of histochemical stain, no product was visible around injuries in the three birds killed immediately following surgery (0-h time-point).

Measurement of Gliosis and Aromatase Expression

When sections stained with the antibody against vimentin were observed with confocal microscopy at low power (5×), the area of reactive glia around needle tract was clearly visible in three sections of the series (note: this represents an anterior–posterior range of ~750 μm). In some of the subjects at 72 h postinsult, a few vimentin cells were observable in a fourth section. However, these were only reliably detectable at high power. Therefore, to infer the area of gliosis, we restricted our measurements to the three sections stained with vimentin in which reactive glia were intense enough to be accurately and reliably observed and measured. We are confident that this represents the middle of the needle tract and (in most subjects) the entirety of the area of reactive gliosis. We present data representing the average area of reactive gliosis based upon these three sections through the middle of reactive gliosis. We captured three images of cells immediately adjacent to mechanical injury per injection per bird at low power (5×, 180 photomicrographs total). For aromatase, we collected three images of labeled cells immediately adjacent to injury per injection per bird at high power (63×, 180 photomicrographs total).

Measurement of Degeneration

When sections stained with Fluoro-Jade B were viewed with confocal microscopy at low power (5 or 10×), degeneration could not be reliably observed and measured because of weak signal fluorescence. At higher power (25×) signal was clearly discernable, however, the halo of degeneration exceeded the frame of the image captured. Therefore, we used high-power images of degeneration in multiple nonoverlapping fields to measure the extent of degeneration away from the needle tract as an index of the WSD. For these measures, we captured 8–10 images per injury per subject at higher power (25×). Images taken were of the area encompassed by degenerating cells adjacent to visible needle tract (always captured in the frame of each picture) in three sections of the series for both the 24- and 72-h time-points. However, at the 2 h, 6 h, 2 and 6 week time-points, we captured images from sections beyond the three used for the 24- and 72-h time-points. We are confident that this represents the middle of needle tract and is an accurate measure of the area of degeneration surrounding injury. We collected a total of 569 photomicrographs and all images were exported and stored as TIFF files.

Data Collection and Analysis

To determine if aromatase inhibition affected reactive gliosis, we measured the area of vimentin immunostaining around each injury. An experimenter blind to the condition of each subject used NIH Image J to render an 8-bit digital version of each vimentin image captured. We measured the area encompassed by injury-induced vimentin positive glia immediately surrounding visible injury tract at low power in three sections representing the medial portion of neural injury to get a measure of the area of reactive gliosis induced by brain insult.

To determine if treatment with fadrozole affected glial aromatase expression, we measured the optical density of immunostain (hereafter: intensity) of aromatase immunoproduct in individual glia surrounding injury. An experimenter blind to the condition of each animal measured the intensity of aromatase immunoproduct in 3–5 glial cells (when detectable) per high-power photomicrograph using NIH Image J. The intensity of unstained areas surrounding aromatase positive glial cells was measured as an index of background and these values were subtracted from the intensity of specific staining to generate a measure of ROD.

To determine the effect of fadrozole on secondary degeneration, we measured the (a) extent of degeneration, (b) the number of dying cells, and (c) the density of degenerating cells. An experimenter blind to the condition of each animal used NIH Image J to render an 8-bit digital version of each Fluoro-Jade B image taken. The threshold of each image was manually adjusted such that the only visible pixels on the screen were Fluoro-Jade B stained cells. Original images in which the thresholds were not adjusted were observed simultaneously to ensure

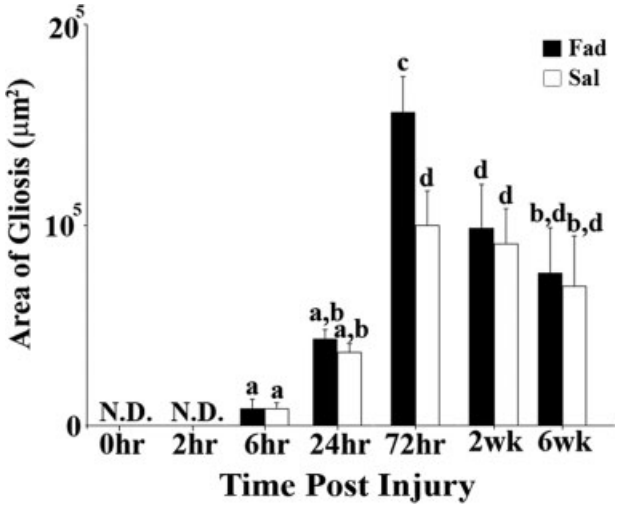

Fig. 1. Histogram representing the mean area of reactive gliosis across time and treatment. Columns with disparate letters are significantly different ($P < 0.05$).

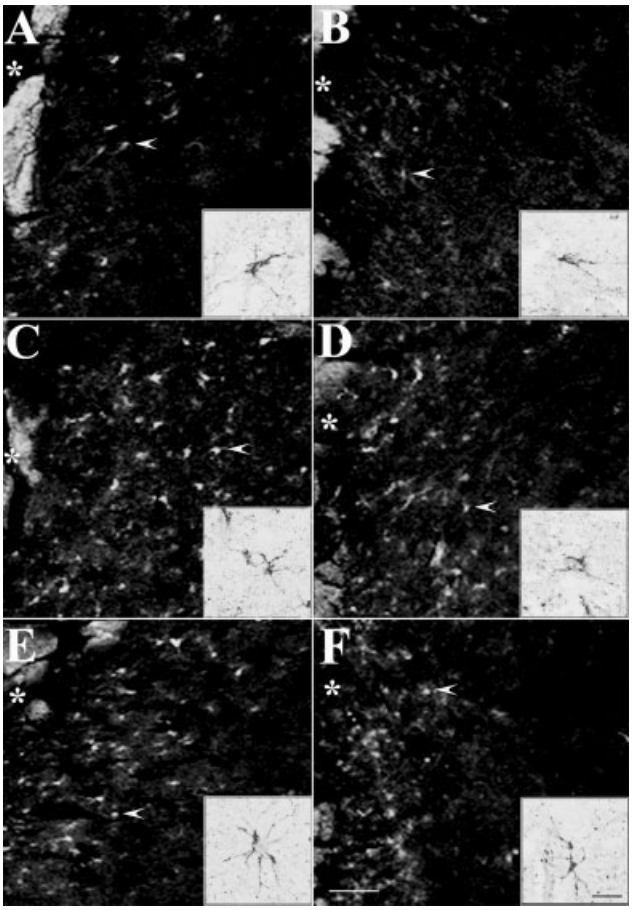

Fig. 2. Vimentin staining in representative subjects at 24 h (**A**, **B**), 72 h (**C**, **D**), and 2 weeks (**E**, **F**) following fadrozole (Fad; A, C, E) and saline (Sal; B, D, F) injury (*). The area of reactive gliosis increased significantly to a maximum 72 h postsaline injury (D) and these levels were sustained up to 6 weeks thereafter. At 72 h postinjury, the area of gliosis was significantly higher around fadrozole injury (C) relative to saline injury (D). Insets are high-power photomicrographs of individual reactive glia neighboring injury (represented by arrowheads in low power images). Scale bar is 100 μm in all low-power photomicrographs and 12.5 μm in all high-power photomicrograph insets. All high-power photomicrograph insets are color inverted images.

accurate cell count and area measures. Parameters were set to count and measure the area of each Fluoro-Jade B positive cell that ranged in size from 25 to 225 μm^2. Visible pixels representing individual Fluoro-Jade B positive cells were counted and following quantification of the number of Fluoro-Jade B positive cells, the area encompassed by these cells (hereafter: extent of degeneration) was measured. The number of Fluoro-Jade B cells was then divided by the extent of degeneration to generate a value of the density of dying cells around each injury. All measures were done using NIH Image J.

Measures of gliosis (vimentin) and degeneration (Fluoro-Jade B) were averaged across injuries and birds. For gliosis and degeneration measures, group means across survival times were analyzed using two-way ANOVA with treatment (fadrozole *vs*. saline) as a within-subject variable and survival time as a between-subjects variable. Tukey-Kramer or Least Square Means tests were used to determine the source of significant variation. For aromatase, we subtracted saline intensity measures from fadrozole intensity measures between hemispheres of the same animal to generate a score of the difference between treatments at each time-point postsurgery. Finally, 95% confidence intervals were computed from these group means and errors [mean ± (1.96 × SEM)] to determine whether the difference between treatments was different from zero.

RESULTS

Reactive Gliosis and Vimentin

We measured the area encompassed by vimentin positive glia around each injury at low power (Figs. 1 and 2).

Relative to the 2-h time-point, we detected an increase in the area of reactive gliosis at 6 h following saline injury. We observed a significant increase in the area of gliosis at 72 h and these levels were sustained up to 6 weeks postsaline insult. Around the fadrozole injury, we found that the area of reactive gliosis increased significantly at 72 h relative to all other time-points measured. The area of reactive gliosis decreased significantly in birds killed 2 weeks following fadrozole injury. We found that the area of reactive gliosis around fadrozole injury was significantly higher relative to saline injury at 72 h postinsult. Specifically, we detected an effect on time-postinjury ($F_{(6,26)} = 13.045$; $P = 0.0001$), treatment ($F_{(1,26)} = 11.743$; $P = 0.0020$) and a significant interaction between time-postinjury and treatment ($F_{(6,26)} = 6.105$; $P = 0.0004$). This effect was because of an increase in the area of reactive gliosis around the 72-h fadrozole injury ($P < 0.05$; Figs. 1 and 2).

Glial Aromatase Expression

The intensity of aromatase immunoproduct is an indirect measure of aromatase activity. A decrease in

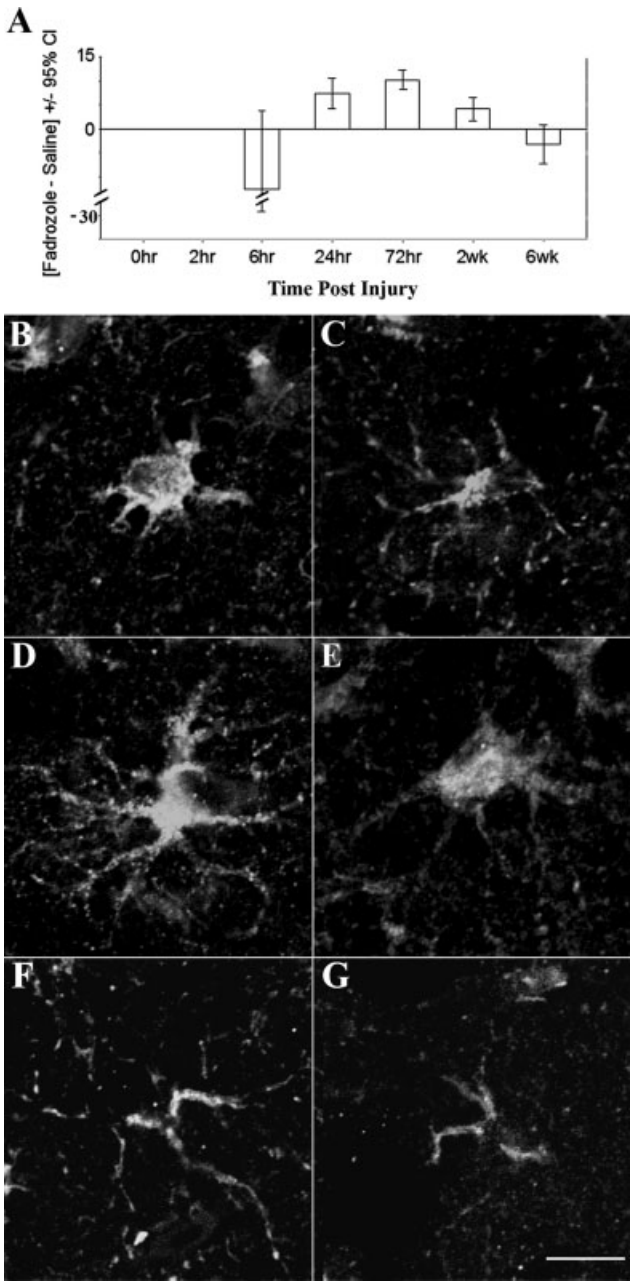

Fig. 3. Histogram representing 95% confidence intervals of group means generated from the subtraction of saline aromatase immunoproduct intensity measures from fadrozole measures (**A**). All positive values represent a higher value in the fadrozole treatment relative to saline. Aromatase staining in representative subjects at 24 h (**B**, **C**), 72 h (**D**, **E**), and 2 weeks (**F**, **G**) following fadrozole (Fad; B, D, F) and saline (Sal; C, E, G) injury. Glial aromatase was first detectable 6 h postinjury, increased significantly to a maximum at 24 h (E), and these levels were sustained up to 6 weeks postsaline injury. Glial aromatase expression was found to be higher around fadrozole injury relative to saline injury at 24 h, 72 h, and 2 weeks postinsult. Scale bar is 12.5 μm and is equal in all photomicrographs.

aromatase activity (via inhibitors like fadrozole) increases aromatase immunoproduct (Harada et al., 1999).

To indirectly infer the amount of aromatase protein in glia, the intensity of glial aromatase immunoproduct was measured on sections containing neural injury due to fadrozole or saline injection (Fig. 3). Glial aromatase was detectable as early as 6 h following saline injury and reached a maximum at 24 h postinsult. Notably, when 95% confidence intervals were computed from group means generated by subtracting saline from fadrozole measures, we found that the 24 h, 72 h, and 2-week time-points were positive values that did not cross zero (see Fig. 3). For this analysis, all positive values represent a higher value in the fadrozole treatment relative to saline treatment. These data suggest that aromatase inhibition was effective as early as 24 h postinsult, remained effective at 72 h, and persisted up to 2 weeks following fadrozole injury.

Fluoro-Jade B and Cellular Degeneration

The marker of cellular degeneration, Fluoro-Jade B, was used to determine if inhibition of glial aromatase affects the dynamics of the WSD following injury to the adult songbird brain (Schmued and Hopkins, 2000).

The extent of degeneration and the number of dying cells significantly increased at 24 and 72 h following fadrozole treatment, after which both of these values decreased back to lower levels. Treatment with fadrozole increased the extent of degeneration ($F_{(1,26)} = 9.546$; $P = 0.0047$) and the number of dying cells ($F_{(1,26)} = 10.019$; $P = 0.0039$) around injury. We discovered an effect of time-postinjury on the extent of degeneration ($F_{(6,26)} = 5.983$; $P = 0.0005$) and the number of dying cells ($F_{(6,26)} = 7.785$; $P = 0.0001$), and a significant interaction between treatment and time-postinjury for both the extent of degeneration and the number of dying cells ($F_{(6,26)} = 6.340$; $P = 0.0003$; $F_{(6,26)} = 8.382$; $P = 0.0001$, respectively). This effect was because of a higher area of degeneration and number of degenerating cells at 24 and 72 h postinjury in the fadrozole treated hemisphere relative to all other data points collected ($P < 0.05$; Figs. 4 and 5).

The area of individual Fluoro-Jade B positive cells, when detectable, did not differ across time-points investigated, but was significantly greater than the 0-h time-point (overall $F_{(6,26)} = 73.004$; $P = 0.0001$). The area of individual Fluoro-Jade B positive cells between treatments ($F_{(1,26)} = 0.570$; $P = 0.4571$) and the interaction between treatment and time-postinjury ($F_{(6,26)} = 0.732$; $P = 0.6282$) were not statistically significant. These data suggest that the size of individual Fluoro-Jade B cells as measured by NIH Image J did not bias measurements of the extent of degeneration, the number of dying cells, or the density of Fluoro-Jade B cells.

The density (number of Fluoro-Jade B positive cells per unit area) of dying cells around each injury was not different around treatment ($F_{(1,26)} = 0.053$; $P = 0.8199$) or the interaction between treatment and time-postinjury ($F_{(6,26)} = 0.209$; $P = 0.9707$). We discovered an effect of time-postinjury on the density of Fluoro-Jade B cells ($F_{(6,26)} = 5.117$; $P = 0.0014$), but this was because of the 0-h time-point being significantly different from all remaining time-points measured ($P < 0.05$; Figs. 4 and 5).

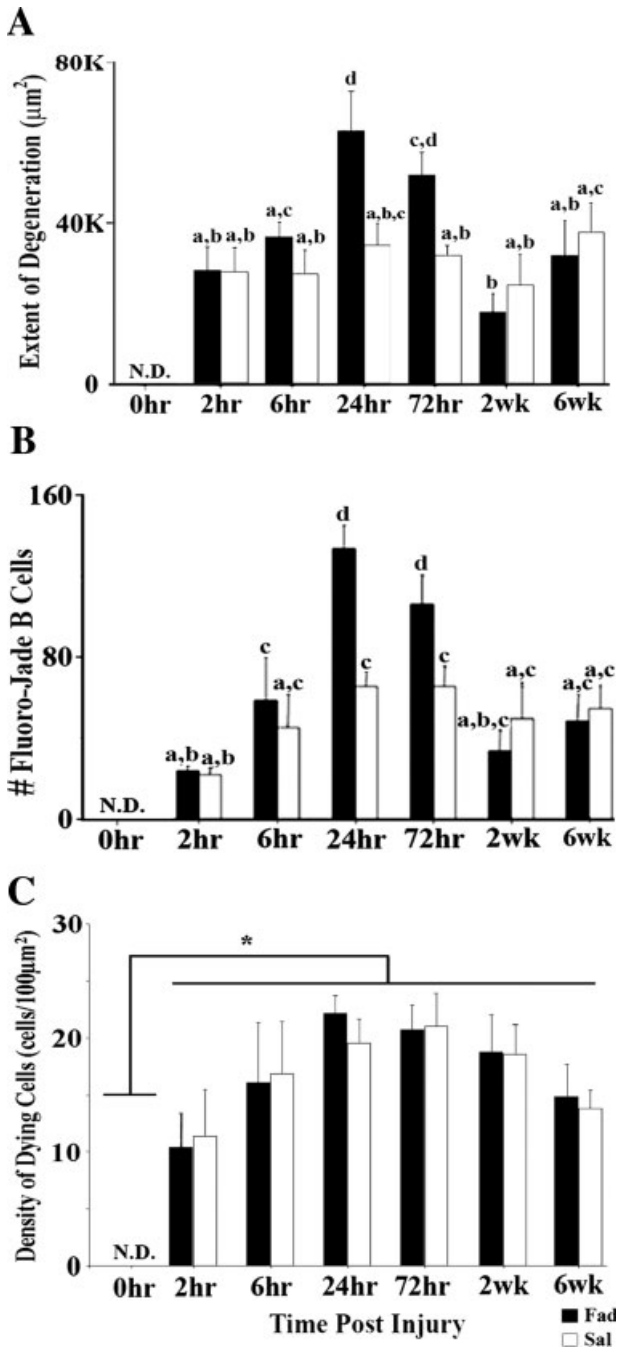

Fig. 4. Histograms representing the mean extent of degeneration (**A**), number of dying cells (**B**), and the density of Fluoro-Jade B cells (C) across time and treatment. Columns with disparate letters are significantly different ($P < 0.05$) in panels (A) and (B). The * in (C) indicates that the 0-h time-point was significantly different from all other time-points.

The manual adjustment of thresholds to measure Fluoro-Jade B did not bias the obtained results. Specifically, thresholds between treatments ($F_{(1,21)} = 6.21E^{-5}$; $P = 0.9938$), time-postinjury ($F_{(5,21)} = 1.336$; $P = 0.2879$), and the interaction between treatment and time-postinjury ($F_{(5,21)} = 1.375$; $P = 0.2736$) did not vary systematically.

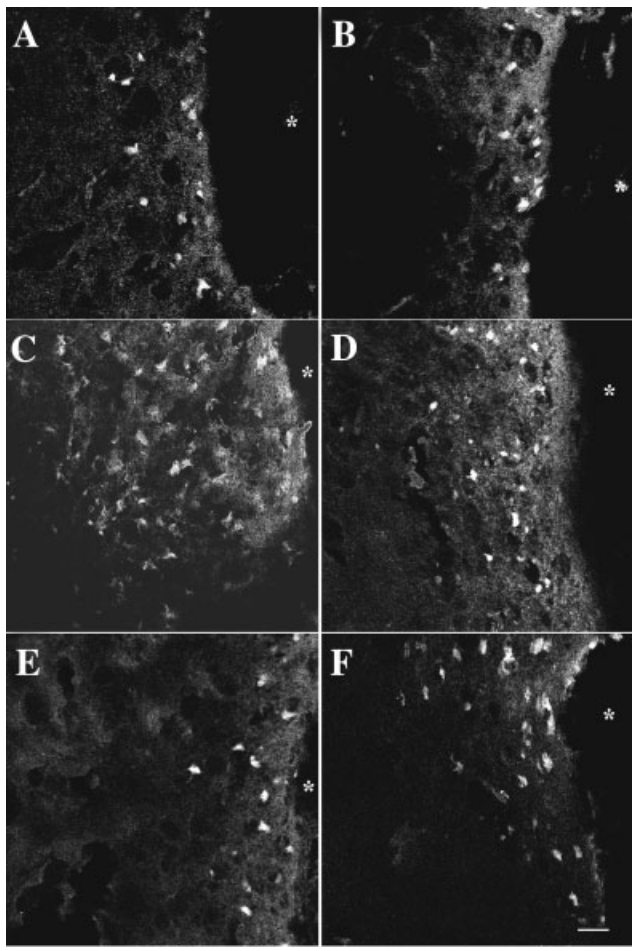

Fig. 5. Fluoro-Jade B staining in representative subjects at 2 h (**A**, **B**), 24 h (**C**, **D**), and 2 weeks (**E**, **F**) following fadrozole (Fad; A, C, E) and saline (Sal; B, D, F) injury (*). While the hemisphere treated with saline did not change in the extent of degeneration, fadrozole treatment increased the extent of degeneration at 24 (C) and 72 h postinjury (not shown) relative to the other time-points investigated. Scale bar is 20 μm and is equal in all photomicrographs.

DISCUSSION

In this study, we examined whether inhibition of glial aromatase affects reactive gliosis and the dynamics of the WSD following injury to the adult songbird brain. We found that inhibition of aromatase increases the area of reactive gliosis following injury to the adult zebra finch brain. Additionally, we found that although degeneration is induced following mechanical injury to the zebra finch telencephalon, this degeneration does not proceed into a WSD as described in mammals (Benkovic et al., 2004; Butler et al., 2002; Sato et al., 2001). A WSD was apparent only following local inhibition of glial aromatase activity. This indicates that glial aromatase is a potent endogenous mitigator of the WSD following neural insult in songbirds. Based upon the time-course of changes following neural injury, it appears that reactive gliosis and aromatase expression may both be consequences of damage to the brain. These data indicate that in songbirds, injury-induced upregulated glial aromatase decreases reactive

gliosis and may be a potent inhibitor of the WSD characteristic of the mammalian brain.

The present data suggest that local aromatization by reactive glia decreases the area of gliosis and secondary degeneration following neural insult. We do not know if these effects reflect direct and independent actions of glial E provision on glial physiology and cellular degeneration, respectively. It is possible that glial aromatization may act to decrease the WSD following neural insult which leads to decreases in reactive gliosis. Conversely, glial aromatization may decrease reactive gliosis and thus, lead to decreases in degeneration. Studies in rats have demonstrated decreases in reactive gliosis following treatment with E (Garcia-Estrada et al., 1993, 1999). At present, the mechanism by which E decreases reactive gliosis following neural injury remains unknown. Additionally, we are unsure as to the precise link between vimentin expression in individual reactive glia and the area of gliosis in songbirds. In mice, recent *in vitro* and *in vivo* studies report decreased astrocytic proliferation and glial scar formation, respectively, following compromise of vimentin expression by injection of RNA antisense to vimentin (Lin and Cai, 2004). These data suggest that vimentin is necessary for normal intermediate filament assembly and glial scar formation following central nervous system insult (Eliasson et al., 1999; Pekny and Nilsson, 2005; Pekny et al., 1999). Whether this is true in the songbird remains to be tested.

Interestingly, the expression of vimentin persists for at least 6 weeks following injury in the songbird brain. The extended time-course of vimentin in the songbird brain suggests a role for glia in brain repair. Injury activated glial cells are a major source of nerve growth factor (Goss et al., 1998) and may assist in axonal growth (Ridet et al., 1997). However, reactive glia may also inhibit neuroplasticity (Fawcett and Asher, 1999). The role reactive gliosis plays 6 weeks postinjury in the adult songbird brain awaits further evaluation.

Passerine glial activation and aromatization following brain damage may be more robust relative to mammals. In the current study, glial aromatase was undetectable for 2 h following injury, which is similar to what is found in rats following middle cerebral artery occlusion (MCAO; Carswell et al., 2005). However, glial aromatase was detectable at 6 h and persisted for 6 weeks following injury to the songbird brain. To the best of our knowledge, the earliest time-point investigated where glial aromatase was detectable in the rodent species is 24 h following MCAO (Carswell et al., 2005). Whether or not glial aromatase is detectable 6 h following injury to the rodent brain remains undetermined. Glial aromatase is detectable 8 days following MCAO (Carswell et al., 2005), 8 days post-kainic acid injection, and 10 days postmechanical lesion in the rodent brain (Garcia-Segura et al., 1999). Glial aromatase was undetectable 30 days post-MCAO in rats (Carswell et al., 2005). The role glial aromatase plays 6 weeks following injury to the adult songbird brain is currently being investigated in our laboratory.

Upregulated aromatase protects against degeneration via the synthesis of E (Azcoitia et al., 2001; Saldanha et al., 2005). The cellular targets employed by locally synthesized E in the songbird brain remains undetermined. In mice, E seems to protect the brain from injury through E receptor (ER)-α rather than ER-β (Dubal et al., 2001). Astroglia upregulate ER-α expression 3 days following injury in rats (Garcia-Ovejero et al., 2002). The plasma membrane-associated E receptor, ER-X, is also upregulated 24 h following injury to the mouse brain (Toran-Allerand et al., 2002). Once bound to a receptor, E may change the expression of several growth factors and/or antiapoptotic genes including brain-derived neurotrophic factor (Amantea et al., 2005), transforming growth factor-β (Buchanan et al., 2000), and the proto-oncogene Bcl-2 (Dubal et al., 1999). E may also interact with insulin-like growth factor-1 receptor and promote neuroprotection (Garcia-Segura et al., 2000). Moreover, cerebral ischemia in the rat brain activates microglia as early as 24 h following insult (Jorgensen et al., 1993), and these microglia are capable of synthesizing androgen receptors (Garcia-Ovejero et al., 2002). The role of microglia following injury to the songbird brain and the cellular and molecular mechanisms used by locally synthesized E in neuroprotection await further testing.

The efficacy of several aromatase inhibitors including fadrozole is reflected in increased aromatase immunoproduct (Harada et al., 1999). Treatment with fadrozole significantly decreases aromatase activity both *in vitro* and *in vivo* in both adult and juvenile telencephalic zebra finch tissue (Saldanha et al., 2004; Wade et al., 1994). In addition, chronic inhibition of aromatase with the nonsteroidal inhibitor R76713 (racemic vorozole) increases the density of aromatase immunoproduct per cell in the adult male quail brain (Balthazart et al., 1992; Foidart et al., 1994). We have previously shown that local inhibition of injury-induced glial aromatase increases aromatase immunoproduct per cell 72 h following fadrozole injury (Wynne and Saldanha, 2004), an effect rescued by simultaneous E injection (Saldanha et al., 2005). In this study, the intensity of glial aromatase immunoproduct around fadrozole injury was higher than that around saline injury as early as 24 h postinjection and lasted up to 2 weeks post-fadrozole injury. These findings suggest that inhibition of glial aromatase activity was effective and lasted $\sim$2 weeks post-fadrozole injection. This is in agreement with studies *in vitro* in which aromatase protein levels increased to about fourfold the control value 24 h following fadrozole treatment (Harada et al., 1999). Additionally, inhibition of aromatase with the nonsteroidal inhibitor vorozole partly increases response latency to a noxious thermal stimulus 2 weeks following treatment in the male Japanese quail (Evrard and Balthazart, 2004). Whether further chronic inhibition of glial aromatase activity or pretreatment with E alters the dynamics of glial aromatase expression and the time-course of cellular degeneration following neural injury remains to be tested.

In mammals, the initiation of a WSD is first detectable as early as 3–12 h following brain injury (Benkovic et al., 2004; Butler et al., 2002; Sato et al., 2001). Secondary degeneration peaks at 24 h postinsult (Benkovic et al.,

2004; Butler et al., 2002; Sato et al., 2001) and declines to control levels 7 days following neural injury (Benkovic et al., 2004; Sato et al., 2001). In contrast to mammals, a WSD was not detected around saline injury in the adult songbird brain. We have previously shown that the number of cells labeled with Fluoro-Jade B, a marker of general degeneration (Schmued and Hopkins, 2000), is not different from the number of cells labeled with TUNEL, a marker for apoptosis, at 72 h postinjury in the zebra finch (Saldanha et al., 2005). Thus, although we cannot be certain that Fluoro-Jade B labeled cells at all time-points in the current study are apoptotic, this hypothesis appears reasonable for cells labeled at the later stages following brain damage. Conversely, the fadrozole-associated injury demonstrated a WSD similar to what is found in the mammalian brain (Benkovic et al., 2004; Butler et al., 2002; Sato et al., 2001). Measures of the extent of degeneration revealed what may be the initiation of a WSD 2 h postinsult followed by a peak in degeneration 24 h post-fadrozole injury. These measures then declined significantly 2 weeks post-fadrozole insult. These data suggest that the upregulation of glial aromatase in the adult zebra finch brain is robust enough to minimize a subsequent WSD following neural insult. Whether (or not) the initiation of a WSD occurs at an earlier time-point remains to be tested.

In summary, the present data strongly suggest that the injury-induced upregulation of glial aromatase in the adult songbird brain is sufficient to decrease reactive gliosis and severely dampen the WSD that is characteristic of the mammalian brain. While the upregulation of glial aromatase in response to mechanical damage does not affect the initiation of the WSD, secondary degeneration is dramatically curtailed by induced aromatase in the zebra finch. These data also provide further evidence that songbirds are excellent models for studying brain damage and repair.

REFERENCES

Alvarez-Buylla A, Buskirk DR, Nottebohm F. 1987. Monoclonal antibody reveals radial glia in adult avian brain. J Comp Neurol 264:159–170.

Amantea D, Russo R, Bagetta G, Corasaniti MT. 2005. From clinical evidence to molecular mechanisms underlying neuroprotection afforded by estrogens. Pharmacol Res 52:119–132.

Anderson KJ, Fugaccia I, Scheff SW. 2003. Fluoro-Jade B stains quiescent and reactive astrocytes in the rodent spinal cord. J Neurotrauma 20:1223–1231.

Arvin B, Neville LF, Barone FC, Feuerstein GZ. 1996. The role of inflammation and cytokines in brain injury. Neurosci Biobehav Rev 20:445–452.

Azcoitia I, Sierra A, Veiga S, Garcia-Segura LM. 2003. Aromatase expression by reactive astroglia is neuroprotective. Ann N Y Acad Sci 1007:298–305.

Azcoitia I, Sierra A, Veiga S, Honda S, Harada N, Garcia-Segura LM. 2001. Brain aromatase is neuroprotective. J Neurobiol 47:318–329.

Balthazart J, Foidart A, Surlemont C, Harada N, Naftolin F. 1992. Neuroanatomical specificity in the autoregulation of aromatase-immunoreactive neurons by androgens and estrogens: An immunocytochemical study. Brain Res 574:280–290.

Balthazart J, Foidart A, Surlemont C, Vockel A, Harada N. 1990. Distribution of aromatase in the brain of the Japanese quail, ring dove, and zebra finch: An immunocytochemical study. J Comp Neurol 301:276–288.

Benkovic SA, O'Callaghan JP, Miller DB. 2004. Sensitive indicators of injury reveal hippocampal damage in C57BL/6J mice treated with kainic acid in the absence of tonic-clonic seizures. Brain Res 1024:59–76.

Benkovic SA, O'Callaghan JP, Miller DB. 2006. Regional neuropathology following kainic acid intoxication in adult and aged C57BL/6J mice. Brain Res 1070:215–231.

Buchanan CD, Mahesh VB, Brann DW. 2000. Estrogen-astrocyte-luteinizing hormone-releasing hormone signaling: A role for transforming growth factor-β(1). Biol Reprod 62:1710–1721.

Butler TL, Kassed CA, Sanberg PR, Willing AE, Pennypacker KR. 2002. Neurodegeneration in the rat hippocampus and striatum after middle cerebral artery occlusion. Brain Res 929:252–260.

Carswell HV, Dominiczak AF, Garcia-Segura LM, Harada N, Hutchison JB, Macrae IM. 2005. Brain aromatase expression after experimental stroke: Topography and time course. J Steroid Biochem Mol Biol 96:89–91.

Chen XH, Siman R, Iwata A, Meaney DF, Trojanowski JQ, Smith DH. 2004. Long-term accumulation of amyloid-β, β-secretase, presenilin-1, and caspase-3 in damaged axons following brain trauma. Am J Pathol 165:357–371.

Chen Y, Swanson RA. 2003. Astrocytes and brain injury. J Cereb Blood Flow Metab 23:137–149.

Clark WM, Walsh CR, Briley DP, Coull BM. 1993. Neutrophil adhesion in central nervous system ischemia in rabbits. Brain Behav Immun 7:63–69.

Darsalia V, Heldmann U, Lindvall O, Kokaia Z. 2005. Stroke-induced neurogenesis in aged brain. Stroke 36:1790–1795.

Dubal DB, Shughrue PJ, Wilson ME, Merchenthaler I, Wise PM. 1999. Estradiol modulates bcl-2 in cerebral ischemia: A potential role for estrogen receptors. J Neurosci 19:6385–6393.

Dubal DB, Zhu H, Yu J, Rau SW, Shughrue PJ, Merchenthaler I, Kindy MS, Wise PM. 2001. Estrogen receptor α, not β, is a critical link in estradiol-mediated protection against brain injury. Proc Natl Acad Sci USA 98:1952–1957.

Eddleston M, Mucke L. 1993. Molecular profile of reactive astrocytes—Implications for their role in neurologic disease. Neuroscience 54:15–36.

Eliasson C, Sahlgren C, Berthold CH, Stakeberg J, Celis JE, Betsholtz C, Eriksson JE, Pekny M. 1999. Intermediate filament protein partnership in astrocytes. J Biol Chem 274:23996–24006.

Eng LF, Ghirnikar RS. 1994. GFAP and astrogliosis. Brain Pathol 4:229–237.

Evrard HC, Balthazart J. 2004. Aromatization of androgens into estrogens reduces response latency to a noxious thermal stimulus in male quail. Horm Behav 45:181–189.

Fawcett JW, Asher RA. 1999. The glial scar and central nervous system repair. Brain Res Bull 49:377–391.

Foidart A, Harada N, Balthazart J. 1994. Effects of steroidal and non steroidal aromatase inhibitors on sexual behavior and aromatase-immunoreactive cells and fibers in the quail brain. Brain Res 657:105–123.

Garcia-Estrada J, Del Rio JA, Luquin S, Soriano E, Garcia-Segura LM. 1993. Gonadal hormones down-regulate reactive gliosis and astrocyte proliferation after a penetrating brain injury. Brain Res 628:271–278.

Garcia-Estrada J, Luquin S, Fernandez AM, Garcia-Segura LM. 1999. Dehydroepiandrosterone, pregnenolone and sex steroids down-regulate reactive astroglia in the male rat brain after a penetrating brain injury. Int J Dev Neurosci 17:145–151.

Garcia-Ovejero D, Azcoitia I, Doncarlos LL, Melcangi RC, Garcia-Segura LM. 2005. Glia-neuron crosstalk in the neuroprotective mechanisms of sex steroid hormones. Brain Res Brain Res Rev 48:273–286.

Garcia-Ovejero D, Veiga S, Garcia-Segura LM, Doncarlos LL. 2002. Glial expression of estrogen and androgen receptors after rat brain injury. J Comp Neurol 450:256–271.

Garcia-Segura LM, Azcoitia I, DonCarlos LL. 2001. Neuroprotection by estradiol. Prog Neurobiol 63:29–60.

Garcia-Segura LM, Cardona-Gomez GP, Chowen JA, Azcoitia I. 2000. Insulin-like growth factor-I receptors and estrogen receptors interact in the promotion of neuronal survival and neuroprotection. J Neurocytol 29:425–437.

Garcia-Segura LM, Veiga S, Sierra A, Melcangi RC, Azcoitia I. 2003. Aromatase: A neuroprotective enzyme. Prog Neurobiol 71:31–41.

Garcia-Segura LM, Wozniak A, Azcoitia I, Rodriguez JR, Hutchison RE, Hutchison JB. 1999. Aromatase expression by astrocytes after brain injury: Implications for local estrogen formation in brain repair. Neuroscience 89:567–578.

Goodson JL, Saldanha CJ, Hahn TP, Soma KK. 2005. Recent advances in behavioral neuroendocrinology: Insights from studies on birds. Horm Behav 48:461–473.

Goss JR, O'Malley ME, Zou L, Styren SD, Kochanek PM, DeKosky ST. 1998. Astrocytes are the major source of nerve growth factor upregula-

tion following traumatic brain injury in the rat. Exp Neurol 149:301–309.
Green PS, Gridley KE, Simpkins JW. 1996. Estradiol protects against β-amyloid (25–35)-induced toxicity in SK-N-SH human neuroblastoma cells. Neurosci Lett 218:165–168.
Harada N, Honda SI, Hatano O. 1999. Aromatase inhibitors and enzyme stability. Endocr Relat Cancer 6:211–218.
Jorgensen MB, Finsen BR, Jensen MB, Castellano B, Diemer NH, Zimmer J. 1993. Microglial and astroglial reactions to ischemic and kainic acid-induced lesions of the adult rat hippocampus. Exp Neurol 120:70–88.
Liberto CM, Albrecht PJ, Herx LM, Yong VW, Levison SW. 2004. Pro-regenerative properties of cytokine-activated astrocytes. J Neurochem 89:1092–1100.
Lin J, Cai W. 2004. Effect of vimentin on reactive gliosis: In vitro and in vivo analysis. J Neurotrauma 21:1671–1682.
Liu D, Smith CL, Barone FC, Ellison JA, Lysko PG, Li K, Simpson IA. 1999. Astrocytic demise precedes delayed neuronal death in focal ischemic rat brain. Brain Res Mol Brain Res 68:29–41.
MacLusky NJ, Naftolin F. 1981. Sexual differentiation of the central nervous system. Science 211:1294–1302.
Mattson MP, Culmsee C, Yu ZF. 2000. Apoptotic and antiapoptotic mechanisms in stroke. Cell Tissue Res 301:173–187.
McGraw J, Hiebert GW, Steeves JD. 2001. Modulating astrogliosis after neurotrauma. J Neurosci Res 63:109–115.
Mize AL, Shapiro RA, Dorsa DM. 2003. Estrogen receptor-mediated neuroprotection from oxidative stress requires activation of the mitogen-activated protein kinase pathway. Endocrinology 144:306–312.
Mrak RE, Griffin WS. 2005. Glia and their cytokines in progression of neurodegeneration. Neurobiol Aging 26:349–354.
Myer DJ, Gurkoff GG, Lee SM, Hovda DA, Sofroniew MV. 2006. Essential protective roles of reactive astrocytes in traumatic brain injury. Brain 129 (Part 10):2761–2772.
Negri Cesi P, Melcangi RC, Celotti F, Martini L. 1992. Aromatase activity in cultured brain cells: Difference between neurons and glia. Brain Res 589:327–332.
Pekny M, Johansson CB, Eliasson C, Stakeberg J, Wallen A, Perlmann T, Lendahl U, Betsholtz C, Berthold CH, Frisen J. 1999. Abnormal reaction to central nervous system injury in mice lacking glial fibrillary acidic protein and vimentin. J Cell Biol 145:503–514.
Pekny M, Nilsson M. 2005. Astrocyte activation and reactive gliosis. Glia 50:427–434.
Peterson RS, Lee DW, Fernando G, Schlinger BA. 2004. Radial glia express aromatase in the injured zebra finch brain. J Comp Neurol 475:261–269.
Peterson RS, Saldanha CJ, Schlinger BA. 2001. Rapid upregulation of aromatase mRNA and protein following neural injury in the zebra finch (*Taeniopygia guttata*). J Neuroendocrinol 13:317–323.
Rau SW, Dubal DB, Bottner M, Gerhold LM, Wise PM. 2003a. Estradiol attenuates programmed cell death after stroke-like injury. J Neurosci 23:11420–11426.
Rau SW, Dubal DB, Bottner M, Wise PM. 2003b. Estradiol differentially regulates c-Fos after focal cerebral ischemia. J Neurosci 23:10487–10494.
Ridet JL, Malhotra SK, Privat A, Gage FH. 1997. Reactive astrocytes: Cellular and molecular cues to biological function. Trends Neurosci 20:570–577.
Saldanha CJ, Rohmann KN, Coomaralingam L, Wynne RD. 2005. Estrogen provision by reactive glia decreases apoptosis in the zebra finch (*Taeniopygia guttata*). J Neurobiol 64:192–201.
Saldanha CJ, Schlinger BA, Micevych PE, Horvath TL. 2004. Presynaptic *N*-methyl-D-aspartate receptor expression is increased by estrogen in an aromatase-rich area of the songbird hippocampus. J Comp Neurol 469:522–534.
Saldanha CJ, Tuerk MJ, Kim YH, Fernandes AO, Arnold AP, Schlinger BA. 2000. Distribution and regulation of telencephalic aromatase expression in the zebra finch revealed with a specific antibody. J Comp Neurol 423:619–630.
Sato M, Chang E, Igarashi T, Noble LJ. 2001. Neuronal injury and loss after traumatic brain injury: Time course and regional variability. Brain Res 917:45–54.
Schlinger BA. 1997. The activity and expression of aromatase in songbirds. Brain Res Bull 44:359–364.
Schmued LC, Hopkins KJ. 2000. Fluoro-Jade B: A high affinity fluorescent marker for the localization of neuronal degeneration. Brain Res 874:123–130.
Shen P, Schlinger BA, Campagnoni AT, Arnold AP. 1995. An atlas of aromatase mRNA expression in the zebra finch brain. J Comp Neurol 360:172–184.
Sofroniew MV. 2005. Reactive astrocytes in neural repair and protection. Neuroscientist 11:400–407.
Stokes TM, Leonard CM, Nottebohm F. 1974. The telencephalon, diencephalon, and mesencephalon of the canary, *Serinus canaria*, in stereotaxic coordinates. J Comp Neurol 156:337–374.
Suzuki S, Brown CM, Wise PM. 2006. Mechanisms of neuroprotection by estrogen. Endocrine 29:209–215.
Swanson RA, Ying W, Kauppinen TM. 2004. Astrocyte influences on ischemic neuronal death. Curr Mol Med 4:193–205.
Toran-Allerand CD, Guan X, MacLusky NJ, Horvath TL, Diano S, Singh M, Connolly ES Jr, Nethrapalli IS, Tinnikov AA. 2002. ER-X: A novel, plasma membrane-associated, putative estrogen receptor that is regulated during development and after ischemic brain injury. J Neurosci 22:8391–8401.
Wade J, Schlinger BA, Hodges L, Arnold AP. 1994. Fadrozole: A potent and specific inhibitor of aromatase in the zebra finch brain. Gen Comp Endocrinol 94:53–61.
Watson RE Jr, Wiegand SJ, Clough RW, Hoffman GE. 1986. Use of cryoprotectant to maintain long-term peptide immunoreactivity and tissue morphology. Peptides 7:155–159.
Wise PM. 2006. Estrogen therapy: Does it help or hurt the adult and aging brain? Insights derived from animal models. Neuroscience 138:831–835.
Wise PM, Dubal DB, Rau SW, Brown CM, Suzuki S. 2005. Are estrogens protective or risk factors in brain injury and neurodegeneration? Re-evaluation after the Women's health initiative. Endocr Rev 26:308–312.
Wynne RD, Saldanha CJ. 2004. Glial aromatization decreases neural injury in the zebra finch (*Taeniopygia guttata*): Influence on apoptosis. J Neuroendocrinol 16:676–683.